(May 19-24 2013 at Makuhari, Chiba, Japan)

©2013. Japan Geoscience Union. All Rights Reserved.



PEM06-01

会場:304

大気重力波の中間圏・下部熱圏への影響について

Effects of Atmospheric Gravity Waves in the Mesosphere-Lower Thermosphere (MLT) Region

津田 敏隆 ^{1*} Toshitaka Tsuda^{1*}

1 京都大学生存圈研究所

¹Research Institute for Sustainable Humanosphere (RISH), Kyoto University

大気重力波は様々な過程により励起され、上方伝搬とともに運動量と力学エネルギーを輸送し、中層大気大循環の駆動ならびに超高層大気における擾乱に深く関係している。ここでは、ラジオゾンデ、流星・MFレーダー等の地上観測およびGPS電波掩蔽データを用いて明らかにされた大気重力波の特性を報告する。特に、中間圏・熱圏下部(MLT) 領域での半年周期振動、あるいはスポラディックE層と大気重力波の相関について議論する。

キーワード: 大気重力波, 流星・MFレーダー, GPS電波掩蔽, 中間圏・下部熱圏, スポラディックE層, 半年周期振動 Keywords: Atmospheric Gravity Waves, Meteor/MF radar, GPS radio occultation, Mesosphere-Lower thermosphere (MLT), Sporadic E layer, Semi-annual oscillation

(May 19-24 2013 at Makuhari, Chiba, Japan)

©2013. Japan Geoscience Union. All Rights Reserved.



PEM06-02

会場:304

Ultra-Fast Kelvin Waves - Sources, Generation of Preferential Modes, and Effects on the Ionosphere-Thermosphere System Ultra-Fast Kelvin Waves - Sources, Generation of Preferential Modes, and Effects on the Ionosphere-Thermosphere System

Uma Das^{1*}, C. J. Pan¹ Uma Das^{1*}, C. J. Pan¹

¹National Central University, Taiwan ¹National Central University, Taiwan

It is known that eastward propagating atmospheric Kelvin waves (KW) are produced due to latent heat release in equatorial regions of deep convections and hence correlate with the outgoing long-wave radiation (OLR). To understand more closely the generation of KW, especially the ultra-fast KW (UFKW), and the relation between KW and OLR, the horizontal and vertical characteristics of UFKW have been investigated from tropopause to stratopause regions and in the thermosphere during 2011 using temperature and electron density data, respectively, obtained from GPS radio occultations by FORMOSAT-3/COSMIC constellation of satellites. Significant amplitudes of UFKW were found in the present investigations in the upper stratosphere (40 to 50 km) during September to November in the temperature retrievals. Simultaneously, the COSMIC electron density retrievals were also investigated and similar periodicities in the ionosphere were found showing the effects of lower atmospheric forcing in the upper atmosphere. We found that the propagation characteristics have little correlation with the mean zonal winds in the stratosphere, i.e., the quasi-biennial oscillation. Also, OLR over the Indonesian region showed very poor correlation with the UFKW amplitudes in contrast to earlier studies. This shows that the generation of UFKW is a more complex phenomenon than known and needs to be addressed in greater detail. Another intriguing aspect is the choice of modes - wavenumber, period, and vertical wavelength. What causes a preferential UFKW to be generated during a particular event? These questions regarding the generation and choice of preferential UFKW will be discussed with more results. How the effects on the ionosphere-thermosphere system depend on the varying characteristics of the UFKW will also be discussed in detail.

 $\neq - \nabla - F$: Ultra-Fast Kelvin Waves, Middle Atmosphere, Ionosphere-Thermosphere Keywords: Ultra-Fast Kelvin Waves, Middle Atmosphere, Ionosphere-Thermosphere

(May 19-24 2013 at Makuhari, Chiba, Japan)

©2013. Japan Geoscience Union. All Rights Reserved.

PEM06-03



時間:5月21日11:35-11:55

Study of low-latitude ionospheric irregularities with the Sanya VHF radar Study of low-latitude ionospheric irregularities with the Sanya VHF radar

Baiqi Ning^{1*}, Guozhu Li¹ Baiqi Ning^{1*}, Guozhu Li¹

¹Institute of Geology and Geophysics, Chinese Academy of Sciences, Beijing 100029, China ¹Institute of Geology and Geophysics, Chinese Academy of Sciences, Beijing 100029, China

A 47.5 MHz VHF radar with a peak power of 24 kW has been set up at Sanya (18.3 N, 109.6 E, dip latitude 12.8 N), China in 2009. The radar can work alternately in coherent scatter and all-sky meteor modes for observing ionospheric irregularities and meteor trails, respectively. In the coherent scatter mode, the radar works like a Doppler coherent backscatter radar to detect ionospheric irregularities. In this study, data from the continuous observations of ionospheric E and F region irregularities are analyzed. It is shown that the daytime E region continuous echoes descend slowly with a descent rate of 1 km/hour, and are highly correlated with the descending of the bottom height of Es trace (hbEs). The Doppler velocity and spectral width of the echoes range from -50 to 25 m/s, and from 20 to 70 m/s, respectively. While at nighttime, the E-region multiple echo layers, echo layer disruption and upper E-region echo layer generation are frequently observed. On the other hand, the radar observations show that the quasi-periodic (QP) echoes occurred above 110 km, and coexisted with E region continuous echo layers. The altitude extent of the QP striations is in a range of about 5-20 km and the duration is about 5-15 minutes. The QP echoes first appeared at higher altitude and then descended to the height close to the continuous echoing region, with a descent rate of 20-30 m/s and a period of about 8 minutes. Further, the Doppler velocities of QP echoes change in time and range and are not related to the striation slop. The zonal drift velocities derived from radar interferometric analysis of QP echoes show apparent variations with altitude. Possible factors responsible for the E region continuous and quasi-periodic echoes are discussed. Additionally, the radar five-beam scanning measurements in east-west direction were used to characterize the longitudinal difference in establishing the initial conditions for equatorial spread-F (ESF) development. Correlative studies between the large scale wave structures (LSWS) and ESF activities are presented. It is shown that the LSWS and ESF have nearly a one-to-one relationship when the F layer undergo an abrupt post-sunset rise (PSSR). However, in the absence of the PSSR, the ESF and GPS scintillation did not always occur following the appearance of LSWS. Sometimes the LSWS events preceded the generation of bottom type spread-F (BSF) that did not develop vertically into ESF and radar plumes. This result may indicate that under inexpressive, weak, or even moderate PSSR conditions, the appearance of the LSWS alone may not be sufficient to produce the post-sunset F region irregularities responsible for ionospheric scintillations.

 $\neq - \mathcal{D} - \mathcal{F}$: Low latitude, Ionospheric irregularities, VHF radar Keywords: Low latitude, Ionospheric irregularities, VHF radar

(May 19-24 2013 at Makuhari, Chiba, Japan)

©2013. Japan Geoscience Union. All Rights Reserved.

PEM06-04



時間:5月21日11:55-12:10

The role of zonal plasma drift for the F-region dynamo: Lunitidal modulation The role of zonal plasma drift for the F-region dynamo: Lunitidal modulation

Jaeheung PARK^{1*}, Hermann LUEHR¹ Jaeheung PARK^{1*}, Hermann LUEHR¹

¹Helmholtz Centre Potsdam, GFZ German Research Centre for Geosciences ¹Helmholtz Centre Potsdam, GFZ German Research Centre for Geosciences

In this study we describe the average zonal drift velocity of F-region plasma (or equivalently, vertical electric field) as derived indirectly from the Challenging Mini-Satellite Payload (CHAMP) observations. Two drivers are known for vertical currents flowing in the equatorial ionospheric F-region: (1) a vertical electric field and (2) the dynamo action of F-region zonal wind. The efficiency of these current drivers depends directly on local Pedersen conductivity. As for CHAMP, we can estimate the vertical current density from the magnetometer, the zonal wind from the accelerometer, and local Pedersen conductivity from a combination of magnetometer/accelerometer/Langmuir-Probe data. In this way the vertical electric field are determined, from which we can deduce the zonal drift velocity of F-region plasma. The obtained velocities are directly compared with the ion drift meter data onboard the Republic of China Satellite-1 (ROCSAT-1). The correlation coefficient between the observed and estimated velocities is about 0.8, the best-fit slope is close to unity, and the best-fit offset is smaller than the range of velocity variations. The result supports the validity of the indirectly estimated zonal velocity. We apply this method to data from a period around a sudden stratospheric warming event during which ionospheric parameters exhibit clear modulations by the lunar tide.

 $\neq - \nabla - F$: equatorial ionosphere, ionospheric dynamo, plasma drift Keywords: equatorial ionosphere, ionospheric dynamo, plasma drift

(May 19-24 2013 at Makuhari, Chiba, Japan)

©2013. Japan Geoscience Union. All Rights Reserved.

PEM06-05



時間:5月21日12:10-12:30

Longitudinal and day-to-day variability in the ionosphere from lower atmosphere tidal forcing Longitudinal and day-to-day variability in the ionosphere from lower atmosphere tidal forcing

Tzu-Wei Fang^{1*}, Rashid Akmaev², Tim Fuller-Rowell¹, Fei Wu¹, Naomi Maruyama¹, George Millward¹ Tzu-Wei Fang^{1*}, Rashid Akmaev², Tim Fuller-Rowell¹, Fei Wu¹, Naomi Maruyama¹, George Millward¹

¹Cooperative Institute for Research in Environmental Sciences, University of Colorado, ²Space Weather Prediction Center, NOAA, Boulder, Colorado, USA.

¹Cooperative Institute for Research in Environmental Sciences, University of Colorado, ²Space Weather Prediction Center, NOAA, Boulder, Colorado, USA.

Simulations with the Global Ionosphere Plasmasphere (GIP) model driven by Whole Atmosphere Model (WAM) winds show significant longitudinal and day-to-day variations in the ionospheric parameters. Under fixed solar and geomagnetic activity levels, the contributions of lower atmosphere tides to the longitudinal and day-to-day variability in the upper atmosphere are estimated. Larger relative variability is found in the nighttime than in the daytime, which is consistent with observations. The perturbations from the lower atmosphere contribute about half of the observed variability in the ionospheric F2 peak density under moderate solar activity and geomagnetic quiet conditions. Simulations also suggest that the wave-4 and wave-3 longitudinal variations in the equatorial vertical drifts during September are dominated by the diurnal eastward propagating non-migrating tides with zonal wave number 3 (DE3) and 2 (DE2), respectively.

 $\neq - \mathcal{P} - \mathcal{F}$: Coupling the lower and upper atmosphere, Ionospheric variability, Longitudinal variation of equatorial ionospherere Keywords: Coupling the lower and upper atmosphere, Ionospheric variability, Longitudinal variation of equatorial ionospherere

(May 19-24 2013 at Makuhari, Chiba, Japan)

©2013. Japan Geoscience Union. All Rights Reserved.

PEM06-06



時間:5月21日12:30-12:45

MIT: a Chinese Space Mission in Pre-study Phase MIT: a Chinese Space Mission in Pre-study Phase

Yong Liu^{1*}, Chi Wang¹, Jiyao Xu¹ Yong Liu^{1*}, Chi Wang¹, Jiyao Xu¹

¹State Key Laboratory of Space Weather, National Space Science Center ¹State Key Laboratory of Space Weather, National Space Science Center

MIT is short for Magnetosphere-Ionosphere-Thermosphere Coupling Constellation Mission. It is designed to study the coupling between magnetosphere, ionosphere and thermosphere. The scientific objective of the mission is to focus on the outflow ions from the ionosphere to the magnetosphere. The constellation is planning to be composed of four spacecrafts, each spacecraft has its own orbit and crosses the polar region at the nearly the same time but at different altitude. With different payloads on-board each spacecraft, we will be able to track the polar upflow ions and study the acceleration mechanism at different altitude. Currently the we are investigating the orbit, the payloads and the strategy for the spacecraft. This phase will end in Oct, 2014, then it will compete for next phase selection.

 $\neq - \nabla - F$: Ion upflow, magnetosphere-ionosphere coupling, space mission Keywords: Ion upflow, magnetosphere-ionosphere coupling, space mission

(May 19-24 2013 at Makuhari, Chiba, Japan)

©2013. Japan Geoscience Union. All Rights Reserved.



PEM06-07

会場:304

中間圏の大気重力波:今後明らかにしたい課題 Gravity waves in the mesosphere: questions to be solved

中村 卓司 ^{1*} Takuji Nakamura^{1*}

1国立極地研究所

¹National Institute of Polar Research

Gravity waves are known to play key role in forming general circulation and latitudinal temperature structure in the middle atmosphere, expecially in the mesosphere and lower thermosphere. It is sometimes stressed that short period gravity waves are more important because of their ability of transporting horizontal momentum upward. However, inertia gravity waves can transport significant amount of kinetic and potential energy and they ctreate turbulent eddy easily, which plays important role of vertical mixing

due to eddy diffusion. In this paper, we re-visit characteristics of internal and inertia gravity waves and propose issue to be solved on gravity wave in the mesosphere and lower thermosphere.

キーワード: 中間圏, 重力波, 中間, 圏, 重力, 波 Keywords: Mesosphere, Gravity Wave, gravity, wave

(May 19-24 2013 at Makuhari, Chiba, Japan)

©2013. Japan Geoscience Union. All Rights Reserved.



PEM06-08

会場:304

全大気モデルを用いた MTI 領域での重力波研究 Gravity Waves in the Mesosphere/Thermosphere/Ionosphere simulated by a Whole Atmosphere Model

三好 勉信^{1*}, 陣 英克², 藤原 均³, 品川 裕之² Yasunobu Miyoshi^{1*}, Hidekatsu Jin², Hitoshi Fujiwara³, Hiroyuki Shinagawa²

1九州大学,2情報通信研究機構,3成蹊大学

¹Kyushu University, ²NICT, ³Seikei University

Behaviors of gravity waves in the thermosphere/ionosphere are examined by using a whole atmosphere model. The dominant period of the simulated gravity waves becomes shorter at higher altitudes due to dissipation processes in the thermosphere, such as molecular viscosity and ion drag force, indicating that gravity waves with a larger horizontal phase velocity (larger vertical wavelength) can penetrate into the thermosphere. We also investigate the longitudinal and seasonal variations of gravity wave activity in low latitudes and upward propagation of gravity waves from the lower atmosphere to the thermosphere/ionosphere. Our results clearly indicate that the longitudinal variation of the gravity wave activity in the mesosphere and thermosphere is closely related to the cumulus convective activity in the tropics. WE are developing a higher horizontal resolution version (about 1 degree longitude by 1 degree latitude) of the atmosphere-ionosphere coupled model (GAIA). Using the high resolution version of the GAIA, we are planning to investigate effects of thermospheric gravity waves on the ionospheric variability.

キーワード: 大気上下結合, 重力波, 数値シミュレーション Keywords: vertical coupling process, gravity wave, numerical simulation

(May 19-24 2013 at Makuhari, Chiba, Japan)

©2013. Japan Geoscience Union. All Rights Reserved.



会場:304



時間:5月21日14:50-15:05

Ionospheric Shock Waves Triggered by Rockets Ionospheric Shock Waves Triggered by Rockets

Charles Lin^{1*}, Jia-Ting Lin¹, Chia Hung Chen¹, Yang-Yi Sun², Jann-Yenq Liu², Yoshihiro Kakinami³, Huixin Liu⁴ Charles Lin^{1*}, Jia-Ting Lin¹, Chia Hung Chen¹, Yang-Yi Sun², Jann-Yenq Liu², Yoshihiro Kakinami³, Huixin Liu⁴

¹Department of Earth Science, National Cheng Kung University, ²Institute of Space Science, National Central University, ³School of Systems Engineering, Kochi University of Technology, ⁴Dept. of Earth and Planetary Science, Faculty of Science, Kyushu University

¹Department of Earth Science, National Cheng Kung University, ²Institute of Space Science, National Central University, ³School of Systems Engineering, Kochi University of Technology, ⁴Dept. of Earth and Planetary Science, Faculty of Science, Kyushu University

This paper present the unprecedented detail of the two-dimensional structure of shock waves resulting from the rocket transit in the upper atmosphere using the time rate change of the total electron content (TEC) derived from dense networks of the groundbased GPS receivers around Japan and Taiwan. From the 2-D TEC maps constructed for the 2009 North Korea Taepoding-2 and 2013 South Korea Naro rocket launces, the V-shape TEC shock wave fronts, with period of 100-600 sec, produced by the propulsive blast of the rocket are seen immediately and propagating perpendicular outward from the rocket trajectory with velocities between 800-1200 m/s. Along the trajectory, clear rocket exhaust depletion of TEC is seen and it propagates northward with a initial velocity of 155 m/s followed by a reduced velocity of 51 m/s, consistent with the background neutral wind predicted by an empirical wind model. After the 10-20 minutes of the rocket transits, the bow and stern waves evolved from the initial blast shock wave front are seen with velocities exceeding 1000 m/s.

 $\neq - \mathcal{D} - \mathcal{F}$: ionospheric shock wave, rocket exhaust depletion of ionospheric TEC Keywords: ionospheric shock wave, rocket exhaust depletion of ionospheric TEC

(May 19-24 2013 at Makuhari, Chiba, Japan)

©2013. Japan Geoscience Union. All Rights Reserved.

PEM06-10

会場:304



時間:5月21日15:05-15:20

630-nm airglow enhancement due to the launch of H-IIA rockets 630-nm airglow enhancement due to the launch of H-IIA rockets

大塚 雄一^{1*}, 塩川 和夫¹, 阿部 琢美² Yuichi Otsuka^{1*}, Kazuo Shiokawa¹, Takumi Abe²

1名古屋大学太陽地球環境研究所,2宇宙航空研究開発機構

¹Solar-Terrestrial Environment Laboratory, Nagoya University, ²Japan Aerospace Exploration Agency

Depletion of the ionospheric plasma density is known to be made by liquid fuel exhausted from rockets. The plasma depletion is considered to be caused by the rapid ion-atom interchange reactions of the ionospheric O^+ with H_2 and H_2O exhausted from rockets, followed by dissociative recombination of the moleculari ions. The current paper reports two evens in which enhancement of 630-nm nightglow were observed after H-IIA rocket launched from Tanegashima, Japan.

An all-sky airglow imager has been operated at Sata, Japan since 2000 as a part of Optical Mesosphere and Thermosphere Imaging system (OMTIs). 630-nm all-sky image is taken with an exposure time of 165 sec and time resolution of 5.5 min. At 1639 UT on May 17, 2012, H-IIA rocket was launched from Tanegashima, Japan. At 1647UT, when the H-IIA rockets reached the ionosphere, an enhancement of the 630-nm airlgow intensity was observed by the airglow imager at Sata. The observed airglow intensity exceeded 2 kR. The airglow enhancement disappeared around 1717 UT. We also analyzed the total electron content (TEC) data obtained from GPS receivers of GNSS receiver network in Japan, and found that the TEC depletion occurred at the same time as the 630-nm airglow enhancement. After another H-IIA rocket was launched at 1117 UT on Sep. 11, 2010, similar 630-nm airglow enhancement due to the gasses exhausted from the rockets.

キーワード: ロケット, 大気光, 電離圏, プラズマ消失 Keywords: rocket, airglow, ionosphere, plasma depletion

(May 19-24 2013 at Makuhari, Chiba, Japan)

©2013. Japan Geoscience Union. All Rights Reserved.

PEM06-11

会場:304



時間:5月21日15:20-15:35

Ionospheric perturbations related to earthquakes Ionospheric perturbations related to earthquakes

柿並 義宏^{1*}, 渡部 重十², 鴨川 仁³ Yoshihiro Kakinami^{1*}, Shigeto Watanabe², Masashi Kamogawa³

¹Kochi University of Technology, ²Hokkaido University, ³Tokyo Gakugei University
 ¹Kochi University of Technology, ²Hokkaido University, ³Tokyo Gakugei University

Ionosphere is disturbed by large earthquakes and tsunamis. When a vertical sudden displacement of the ground and sea surface caused by the earthquake and tsunami excites acoustic and gravity waves in the atmosphere, the acoustic and gravity waves propagate into the ionosphere and disturb ionospheric plasma. The M 9.0 Tohoku earthquake (Tohoku EQ) was a megathrust-type which occurred on March 11 of 2011 at 0546 UT in the western Pacific Ocean. After the Tohoku EQ, many types of ionospheric disturbances such as acoustic resonance and gravity wave were observed. Furthermore, large plasma depletion named "tsunamigenic ionospheric hole" was observed. Similar plasma deletions were also found in the 2010 M8.8 Chile and the 2004 M9.1 Sumatra earthquakes. This occurs because plasma is descending at the lower thermosphere where the recombination of ions and electrons is high through the meter-scale downwelling of sea surface at the tsunami source area, and is highly depleted due to the chemical processes.

We also found a faster CID propagated at ~3.0 km/s only in the west-southwest, while a slower CID propagated concentrically at 1.2 km/s or slower from the tsunami source area in the Tohoku EQ. Taking the propagation speed and oscillation cycle into account, the faster CID was associated with a Rayleigh wave but the slower CID was associated with an acoustic or gravity wave. The north-south asymmetry of the CID associated with the Rayleigh wave suggests that the Rayleigh wave did not act as a point source of the acoustic wave because a point source propagating in all directions produces CID in all directions. Therefore, a superimposed wave front of acoustic waves excited by the Rayleigh wave produced the north-south asymmetry of the faster CID due to the magnetic inclination effect.

 $\neq - \nabla - \beta$: ionospheric disturbance, GPS-TEC, earthquake, Rayleigh wave, acoustic wave, ionospheric hole Keywords: ionospheric disturbance, GPS-TEC, earthquake, Rayleigh wave, acoustic wave, ionospheric hole

(May 19-24 2013 at Makuhari, Chiba, Japan)

©2013. Japan Geoscience Union. All Rights Reserved.

PEM06-12





時間:5月21日15:35-15:50

Possible relationship between Solar Wind Input Energy and Seismicity Possible relationship between Solar Wind Input Energy and Seismicity

Mohamad Huzaimy Bin Jusoh^{1*}, Huixin Liu², Kiyohumi Yumoto² Mohamad Huzaimy Bin Jusoh^{1*}, Huixin Liu², Kiyohumi Yumoto²

¹Department of Earth and Planetary Sciences, Graduate School of Sciences, Kyushu University, ²Department of Earth and Planetary Science, Kyushu University and ICSWSE, Kyushu University

¹Department of Earth and Planetary Sciences, Graduate School of Sciences, Kyushu University, ²Department of Earth and Planetary Science, Kyushu University and ICSWSE, Kyushu University

Solar wind is one of the most prominent features in interplanetary magnetic field (IMF) and acts as a medium for most of solar perturbations to penetrate into the earth ionosphere. The connection of solar wind and magnetosphere to the ionosphere has been introduced since early year 1960 by considering the solar wind energy transfer or input energy as a function of solar wind parameters. This energy can cause several space weather events such as aurora, geomagnetic storm and ionospheric disturbances. In this paper, we investigate possible influence of solar wind input energy on earthquake events. Our previous statistical analysis on relationship between solar and seismic activities (Jusoh and Yumoto, 2011, Jusoh et al., 2012) has shown high tendency of earthquakes during lower phase solar cycles. However a clear coupling mechanism was not established yet. To connect the solar impact on seismicity, we investigate the penetration of solar wind energy to lower ionosphere and lithosphere during high solar wind events. In our analysis, the underground polarization ratios for Pc3-5 were analyzed with the occurrence of local earthquake events at certain time periods. This analysis focuses at Onagawa area, which is one of major seismic regions in Japan.

Solar wind parameters were obtained from the Goddard Space Flight Center, NASA via the OMNIWeb Data Explorer and the Space Physics Data Facility. Earthquake events were extracted from the Advanced National Seismic System (ANSS) database. The localized Pc3-Pc5 magnetic pulsations for polarization ratio data were extracted from Magnetic Data Acquisition System (MAGDAS)/Circum Pan Magnetic Network (CPMN) located at Onagawa station, Japan (N38.43, E141.47). This magnetometer array has been established by International Center for Space Weather Science and Education, Kyushu University, Japan.

From the results, we observed significant correlations between solar wind input energy and underground polarization ratio at difference earthquake magnitudes and epicenter depths. The details of the analysis will be discussed in the presentation.

 $\neq - \nabla - F$: High Speed Solar Wind, Solar Wind Input Energy, Geomagnetic Pulsation, Underground Polarization ratio, Earthquake

Keywords: High Speed Solar Wind, Solar Wind Input Energy, Geomagnetic Pulsation, Underground Polarization ratio, Earthquake

(May 19-24 2013 at Makuhari, Chiba, Japan)

©2013. Japan Geoscience Union. All Rights Reserved.



会場:304



時間:5月21日16:15-16:30

Nighttime electron density enhancements in East Asia Nighttime electron density enhancements in East Asia

Libo Liu^{1*}, Yanyan Zhang¹, Weixing Wan¹, Baiqi Ning¹ Libo Liu^{1*}, Yanyan Zhang¹, Weixing Wan¹, Baiqi Ning¹

¹CAS Key Laboratory of Ionospheric Environment, Institute of Geology and Geophysics, Chinese Academy ¹CAS Key Laboratory of Ionospheric Environment, Institute of Geology and Geophysics, Chinese Academy

The critical frequency of F2-layer (foF2) and other ionosonde data observed at stations, Okinawa, Yamagawa, Kokubunji, Wakkanai, and Sanya in East Asia sector have been collected to study the nighttime behavior of ionospheric F layer at middle and low latitudes. Enhancements in nighttime electron density are frequently present at these stations in pre-midnight and post-midnight intervals. The results show obvious seasonal and solar activity dependencies in the pattern of the nighttime ionospheric electron density enhancements. The pre-midnight enhancements have larger occurrence probability in summer months than in winter months, and the post-midnight enhancements have an opposite trend: more likely in winter months than in summer months. Nighttime enhancement in electron density tends to occur under lower solar activity. Analysis reveals that the effect of neutral winds is in reasonable agreement with the seasonal and solar activity variations of the nighttime electron density enhancements.

Acknowledgements: Ionosonde data are provided from BNOSE of IGGCAS and National Institute of Information and Communications Technology. This research was supported by the projects of Chinese Academy of Sciences (KZZD-EW-01-3), National Key Basic Research Program of China (2012CB825604), and National Natural Science Foundation of China (41174137 and 41231065).

 $\neq - \nabla - F$: ionosphere, nighttime enhancement, low latitude Keywords: ionosphere, nighttime enhancement, low latitude

(May 19-24 2013 at Makuhari, Chiba, Japan)

©2013. Japan Geoscience Union. All Rights Reserved.

PEM06-14

会場:304



時間:5月21日16:30-16:45

East-west differences in F-region electron density at midlatitude: comparision between the US and the Far East regions East-west differences in F-region electron density at midlatitude: comparision between the US and the Far East regions

Biqiang Zhao^{1*} Biqiang Zhao^{1*}

¹INSTITUTE OF GEOLOGY AND GEOPHYSICS CHINESE ACADEMY OF SCIENCES ¹INSTITUTE OF GEOLOGY AND GEOPHYSICS CHINESE ACADEMY OF SCIENCES

The global configuration of the geomagnetic field shows that the maximum east-west difference in geomagnetic declination of northern middle latitude lies in the US region (about 32 degree), which produces the significant ionospheric east-west coast difference in terms of total electron content (TEC) first revealed by Zhang et al. [2011]. For verification, it is valuable to investigate this feature over the Far East area where also shows significant geomagnetic declination east-west gradient but smaller (about 15 degree) than that of US. The current study provides evidence of the longitudinal change supporting the thermospheric zonal wind mechanism by examining the climatology of peak electron density (NmF2), electron density (Ne) of different altitudes in the Far East regions with a longitude separation of up to 40-60 degree based on ground ionosonde and space-based measurements. Although the east-west difference (Rew) over the Far East area displays a clear diurnal variation similar to the US feature, that is negative Rew (West Ne > East Ne) in the noon and positive at evening-night, the observational results reveal more differences including: 1) The noontime negative Rew is most pronounced in April-June while in US during February-March. Thus for the late spring and summer period negative Rew over the Far East region is more significant than that of US. 2) The positive Rew at night is much less evident than in US, especially without winter enhancement. 3) The magnitude of negative Rew tends to enhance toward solar maximum while in US showing anti-correlation with the solar activity. The altitude distribution of pronounced negative difference (300~400 km) moves upward as the solar flux increases and hence produces the different solar activity dependence at different altitude. The result in the paper is not simply a comparison corresponding to the US results but raises some new features that are worth further study and improve our current understanding of ionospheric longitude difference at midlatitude.

 $\neq - \nabla - F$: middle latitude ionosphere, east-west difference, Far East region Keywords: middle latitude ionosphere, east-west difference, Far East region

(May 19-24 2013 at Makuhari, Chiba, Japan)

©2013. Japan Geoscience Union. All Rights Reserved.

PEM06-15



時間:5月21日16:45-17:00

Ionospheric response to high-speed streams at solar minimum Ionospheric response to high-speed streams at solar minimum

Jing Liu^{1*}, Libo Liu¹ Jing Liu^{1*}, Libo Liu¹

¹INSTITUTE OF GEOLOGY AND GEOPHYSICS CHINESE ACADEMY OF SCIENCES ¹INSTITUTE OF GEOLOGY AND GEOPHYSICS CHINESE ACADEMY OF SCIENCES

To demonstrate high-speed stream effects during the recent deep solar minimum year 2008, we have analyzed manually scaled foF2 and hmF2 at Jicamarca and total electron content (TEC) in the equatorial ionization anomaly (EIA) region over the America longitudinal sector. Our results reveal that a prominent 9-day oscillation appears in the hmF2 and foF2 at the dip equator. The 9-day oscillation amplitudes of foF2 are not always positively correlated with TEC in the equatorial ionosphere and they show non-linear dependence on the intensity of geomagnetic disturbances. With the outputs of Fejer and Scherliess [1997] empirical model, we found that this periodicity is also present in equatorial vertical drifts caused by disturbance dynamo electric field (DDEF) but absent in the drifts due to prompt penetration electric field (PPEF). DDEF effects on the equatorial periodic variations alone are not sufficient to explain the observed phenomena; other mechanisms, such as thermal expansion/contraction and neutral composition changes, are also the plausible causes of the periodic oscillation in the equatorial ionosphere. Further, the complicated patterns appear in the 9-day band-pass-filtered TEC perturbations in the EIA region, and they are quite different from the patterns of global coherent thermospheric oscillations triggered by high-speed streams. We also found that the latitudinal variations of band-passed-filtered TEC present different behaviors involving tilt latitudinal configuration, anti-phased correlation between the crests and trough, and south-north asymmetry, which vary as a function of season, local time, or even from event to event.

(May 19-24 2013 at Makuhari, Chiba, Japan)

©2013. Japan Geoscience Union. All Rights Reserved.



PEM06-16

会場:304

プラズマバブルと電離圏全電子数空間勾配の関係について Relationship between plasma bubbles and spatial gradient in ionospheric TEC

斎藤 享^{1*}, 吉原 貴之¹, 大塚 雄一² Susumu Saito^{1*}, Takayuki Yoshihara¹, Yuichi Otsuka²

1 電子航法研究所, 2 名古屋大学太陽地球環境研究所

¹Electronic Navigation Research Institute, ²STEL, Nagoya University

The ionosphere is one of the serious error source in global navigation satellite systems (GNSS). Spatial gradients in ionospheric total electron contents (TEC) makes it difficult to correct ionosphere induced error by differential GNSS techniques.

Plasma bubbles are known to accompany sharp TEC gradient. Its frequent occurrence is a serious issue in advanced applications of GNSS. Plasma bubbles includes plasma irregularities with various scale sizes and the correspondence between the large scale plasma depletion and the sharp TEC gradient is not clear.

In this study, spatial gradients in TEC are observed by five GNSS receivers distributed with distances 0.4-1.6 km at Ishigaki (about 20 deg. magnetic latitude), Japan. Large scale plasma depletions are observed by an all-sky airglow imager located at Yonaguni (about 100 km west of Ishigaki). Detailed comparison between the TEC gradients and airglow intensity maps are conducted to reveal where the sharp TEC gradients exist in plasma bubbles.

Keywords: Plasma bubble, Ionospheric TEC, Spatial gradient in TEC, Lows latitude ionosphere, GNSS

(May 19-24 2013 at Makuhari, Chiba, Japan)

©2013. Japan Geoscience Union. All Rights Reserved.

PEM06-17



時間:5月21日17:15-17:30

観測・GCM シミュレーションによる極域超高層大気の研究 Studies of the polar upper atmosphere from observations and GCM simulations

藤原 均^{1*}, 野澤 悟徳², 小川 泰信³, 三好 勉信⁴, 陣 英克⁵, 品川 裕之⁵ Hitoshi Fujiwara^{1*}, Satonori Nozawa², Yasunobu Ogawa³, Yasunobu Miyoshi⁴, Hidekatsu Jin⁵, Hiroyuki Shinagawa⁵

1 成蹊大学 理工学部, 2 名古屋大学 太陽地球環境研究所, 3 国立極地研究所, 4 九州大学 大学院理学研究院, 5 情報通信研究 機構

¹Faculty of Science and Technology, Seikei University, ²Solar Terrestrial Environment Laboratory, Nagoya University, ³National Institute of Polar Research, ⁴Department of Earth and Planetary Sciences, Faculty of Sciences, Kyushu University, ⁵National Institute of Information and Communications Technology

Various types of ionospheric and thermospheric variations, which would result from the solar phenomena, e.g, the solar flare/CME, have been found from various ground-based and satellite observations. However, details of the variations of the polar cap ionosphere, thermospheric wind and density variations are still unknown because we have little understanding of energy inputs into the polar thermosphere/ionosphere. Recent satellite observations, e.g., CHAMP observations, have revealed thermospheric density variations caused by significant solar energy injection into the polar themosphere and ionosphere. Some IS radar observations also have revealed ionospheric signatures of energy inputs into the polar region due to changes in the solar wind. Comprehensive studies by observations from space, ground-based ones, and numerical simulations will enable us to understand the polar thermosphere and ionosphere quantitatively. In order to understand variations of the polar ionosphere from the solar minimum to maximum periods, we have made EISCAT experiments in January 2011, March, 2012, and March 2013. For example, ionospheric variations were observed during solar flare and CME events on March 12, 2012. These EISCAT data clearly show an example of the solar wind, magnetosphere, and ionosphere coupling. In addition to the EISCAT observations, we will also investigate variations of the polar thermosphere during periods of significant solar activities from GCM simulations.

キーワード:熱圏,電離圏,極域,太陽風

Keywords: thermosphere, ionosphere, polar region, solar wind

(May 19-24 2013 at Makuhari, Chiba, Japan)

©2013. Japan Geoscience Union. All Rights Reserved.



会場:304



時間:5月21日17:30-17:45

昼側カスプ域付近の熱圏質量密度異常の新しい生成機構 New mechanisms of thermospheric mass density anomaly around the dayside cusp region

松村充^{1*},田口聪² Mitsuru Matsumura^{1*}, Satoshi Taguchi²

1 電気通信大学 宇宙・電磁環境研究センター, 2 電気通信大学 情報理工学研究科

¹Center for Space Science and Radio Engineering, University of Electro-Communications, ²Graduate School of Informatics and Engineering, University of Electro-Communications

CHAMP satellite observations have revealed that the thermospheric mass density statistically enhances in the cusp region. In this presentation we provide new mechanisms of the density anomaly. A numerical model of nonhydrostatic and compressible atmosphere coupled with ionosphere is used to investigate the response to a 2-cell convection pattern in ion distribution produced by only solar EUV. It is found that vertical upwelling and horizontal compression of neutral air around the cusp at 400 km altitude result in the neutral density anomaly. The upwelling is caused by heat transfer from ions to neutrals. Distribution of ion drift velocity and ion density naturally confines the region of the highest heating rate to the cusp. The compression is caused by horizontal momentum transfer from ions to neutrals. Ion drag and the resultant neutral flow converge at terminator near the cusp. Both of the mechanisms provide a causal explanation of seasonal variation, solar wind and solar EUV dependences of the density anomaly.

Keywords: cusp, thermospheric mass density anomaly, CHAMP satellite

(May 19-24 2013 at Makuhari, Chiba, Japan)

©2013. Japan Geoscience Union. All Rights Reserved.

PEM06-19

会場:304



時間:5月21日17:45-18:00

Strom-time characteristics of 630 nm airglow intensity associated with polar-cap patches Strom-time characteristics of 630 nm airglow intensity associated with polar-cap patches

坂井 純¹*, 細川 敬祐¹, 田口 聪¹, 小川 泰信² Jun Sakai¹*, Keisuke Hosokawa¹, Satoshi Taguchi¹, Yasunobu Ogawa²

1 電気通信大学, 2 国立極地研究所

¹University of Electro-Communications, ²National Institudte of Polar Research

Observing the optical intensity of 630 nm airglow (I_{630}) radiated from polar cap patches with all-sky imagers is an important method to understand the dynamics of the F-region ionosphere at polar latitudes. A series of all-sky images provides information about spatial distribution of electron density structures and their motion as well as relative magnitude of F region electron density. To interpret these data quantitatively we need to know the height profile of airglow emission, namely the volume emission rate (V_{630}), which cannot be obtained by ground-based optical measurement. It is known that I_{630} is proportional to the peak electron density of the F region (NmF2) but is inversely correlated to the height of the F region peak (hmF2). This suggests that some ionosonde or incoherent scatter radar observations of NmF2 and hmF2 inside the field of view (FOV) of an all-sky imager may help us estimate the height profile of V_{630} over the FOV of the imager. However, since V_{630} is largely dependent on neutral gas profiles, particularly on molecular oxygen (O_2) and molecular nitrogen (N_2) profiles, it is not easy to estimate the peak emission height from regular ionospheric observations. Furthermore, during a disturbed period, when both neutral gases and the ionosphere are significantly lifted, estimating the emission height can be more complicated.

In this study, we examine the optical intensity of 630 nm airglow associated with polar cap patches during a magnetic storm that occurred on 22 January 2012. Optical intensity is measured by an all sky imager located at Longyearbyen, Svalbard. The time variation of the optical intensity is compared with the time variation of the F-region electron density observed by the EISCAT Svalbard Radar (ESR). The observed I_{630} variation is in good agreement with the NmF2 variation, and I_{630} is inversely correlated with the hmF2, which is consistent with the known relationship between I_{630} , NmF2 and hmF2. To estimate the height profile of V_{630} we adopt a simple V_{630} model using MSIS-modelled neutral gas profiles and IRI-modelled O⁺ ion profile. Optical intensity is calculated by height-integrating the V_{630} and the result is in good agreement with the observation. The modelled V_{630} calculations for several magnetic storms, ranging from $D_{st}=0$ nT to -400 nT, revealed that (1) I_{630} is strongly affected by scale heights of molecular gases, (2) peak V_{630} height is determined by F region height but usually lower than hmF2, and (3) under disturbed conditions lifted O_2 tends to enhance V_{630} while lifted N_2 tends to quench it, and the overall outcome is increased I_{630} . This set of conclusions indicates that special care, in particular for the height profiles of ionized and neutral densities, must be taken when we interpret airglow observations during severe magnetic storms.

 $\neq - \nabla - F$: polar cap patch, 630 nm airglow, ionosphere, magnetic storm Keywords: polar cap patch, 630 nm airglow, ionosphere, magnetic storm

(May 19-24 2013 at Makuhari, Chiba, Japan)

©2013. Japan Geoscience Union. All Rights Reserved.

PEM06-20



時間:5月22日09:00-09:20

The longitudinal variation in daily mean thermospheric mass density The longitudinal variation in daily mean thermospheric mass density

Jiyao Xu^{1*}, Wenbin Wang², Hong Gao¹ Jiyao Xu^{1*}, Wenbin Wang², Hong Gao¹

¹State Key Laboratory of Space Weather, Center for Space Science and Applied research, CAS, China., ²High Altitude Observatory, National Center for Atmospheric Research, Boulder, CO 30307, USA.

¹State Key Laboratory of Space Weather, Center for Space Science and Applied research, CAS, China., ²High Altitude Observatory, National Center for Atmospheric Research, Boulder, CO 30307, USA.

In this work, we use thermosphere mass density data inferred from the accelerometer measurements made by the GRACE (480 km) and CHAMP (380 km) satellites to study the longitude structure of the daily mean thermospheric mass density under the quiet geomagnetic condition (Ap<10). Daily mean is performed on these data so that the effects of tides are removed. The results show that the thermospheric mass density is not uniform in the zonal direction, and there are strong longitude variations at all latitudes. The maximum of the daily mean mass density is always around the aurora zone which suggests that these longitudinal variations are most likely the result of auroral heating which includes Joule and particle heating. The largest relative longitudinal changes of the daily mean thermospheric mass density occur at high latitudes from October to February in the northern hemisphere and from March to September in the southern hemisphere. The high density regions extend toward lower latitudes and even into the opposite hemisphere. This extension is mainly confined to the longitudes where the magnetic poles are located. Thus the relative changes of the daily mean thermospheric mass density have strong seasonal variations and show an annual oscillation at high and middle latitudes but a semi-annual oscillation around the equator. There is asymmetry between two hemispheres in the longitude variations in the thermospheric mass density: they are stronger in southern hemisphere than in northern hemisphere. The mass density data observed by the GARCE and CHAMP satellites between 2003 and 2008 show similar characteristics at the two different altitudes.

 $\neq - \nabla - F$: thermosphere, auroral heating, Joule and particle heating, The longitudinal variation Keywords: thermosphere, auroral heating, Joule and particle heating, The longitudinal variation

(May 19-24 2013 at Makuhari, Chiba, Japan)

©2013. Japan Geoscience Union. All Rights Reserved.

PEM06-21



時間:5月22日09:20-09:35

Ionospheric Response to Stratospheric Sudden Warming Studied by Realistic Whole Atmosphere Ionosphere Coupled Simulation Ionospheric Response to Stratospheric Sudden Warming Studied by Realistic Whole Atmosphere Ionosphere Coupled Simulation

陣 英克^{1*}, 三好 勉信², Liu Huixin², 藤原 均³, 品川 裕之¹ Hidekatsu Jin^{1*}, Yasunobu Miyoshi², Huixin Liu², Hitoshi Fujiwara³, Hiroyuki Shinagawa¹

1情報通信研究機構,2九州大学,3成蹊大学

¹NICT, ²Kyushu University, ³Seikei University

It has been known recently that the effects of stratospheric sudden warming (SSW) appear not only within the middle atmosphere but extend even to the upper atmosphere. SSW itself is known to occur as a result of the interaction between the upward propagating planetary waves and background meridional circulation. The interaction basically occurs in the polar stratosphere. On the other hand, recent observation and modeling studies have shown that tidal property at low latitudes as well as global thermal structure change in the upper atmosphere in response to stratospheric warming. Physical processes have not been established yet for the connection between the polar stratosphere and the upper atmospheric variations. In this study, we utilized a whole atmosphere-ionosphere coupled model, named as Ground-to-topside model of Atmosphere and Ionosphere for Aeronomy (GAIA). The model has recently assimilated meteorological reanalysis data (JRA25, provided by Japanese Meteorological Agency) so it could reproduce upper atmosphere driven by realistic lower atmosphere. The comparison of the model result with satellite observations has shown that the model successfully reproduces general features from the drastic change of the polar middle atmosphere as its response. The detail analysis of the model result has revealed that the ionospheric variations are mainly caused by the (2, 2) and (2, 3) modes of the semidiurnal migrating tide which originally enhanced in the middle atmosphere due to the change in the global circulation. Cases of other SSWs are also studied.

キーワード: 成層圏突然昇温, モデリング, 電離圏, 熱圏, 中層大気, 大気潮汐

Keywords: stratospheric sudden warming, modeling, ionosphere, thermosphere, middle atmosphere, atmospheric tide

(May 19-24 2013 at Makuhari, Chiba, Japan)

©2013. Japan Geoscience Union. All Rights Reserved.

PEM06-22



時間:5月22日09:35-09:50

Upper atmosphere response to stratosphere sudden warming: local time and height dependence simulated by GAIA model Upper atmosphere response to stratosphere sudden warming: local time and height dependence simulated by GAIA model

Huixin Liu^{1*}, Hidekatsu Jin², Yasunobu Miyoshi¹, Hitoshi Fujiwara³, Hiroyuki Shinagawa² Huixin Liu^{1*}, Hidekatsu Jin², Yasunobu Miyoshi¹, Hitoshi Fujiwara³, Hiroyuki Shinagawa²

¹Kyushu University, Japan, ²NICT, Japan, ³Seikei University, Japan ¹Kyushu University, Japan, ²NICT, Japan, ³Seikei University, Japan

The whole atmosphere model GAIA is employed to shed light on atmospheric response to the 2009 major stratosphere sudden warming (SSW) from the ground to exobase. Distinct features are revealed about SSW impacts on thermospheric temperature and density above 100 km altitude. 1. The effect is primarily quasi-semidiurnal in tropical regions, with warming in the noon and premidnight sectors and cooling in the dawn and dusk sectors.2. This pattern exists at all altitudes above 100 km, with its phase being almost constant above 200 km, but propagates downward in the lower thermosphere between 100-200 km. 3. The northern polar region experiences warming in a narrow layer between 100 - 130 km, while the southern polar region experiences cooling throughout 100 - 400 km altitudes. 4. The global net thermal effect on the atmosphere above 100 km is a cooling of about -12 K. These characteristics provide us with an urgently needed global context to better connect and understand the increasing upper atmosphere observations during SSW events.

 $\neq - \nabla - F$: Thermosphere temperature, Stratosphere Sudden warming, vertical coupling Keywords: Thermosphere temperature, Stratosphere Sudden warming, vertical coupling

(May 19-24 2013 at Makuhari, Chiba, Japan)

©2013. Japan Geoscience Union. All Rights Reserved.



時間:5月22日09:50-10:05

2009年1月の成層圏突然昇温の北半球電離圏への影響 Response of northern hemisphere ionosphere to 2009 January SSW

小山 孝一郎^{1*}, 周 中亭², 佳廷 林², 許 美蘭³, 呉 宣軒², 劉⁴, 林 建宏², 湯元清文⁴ Koichiro Oyama^{1*}, Jhong-Ting Chou², Jia-Ting Lin², Mei- lan Hsue³, Yi Syuan Wu², Huixing Liu⁴, Charles Lin², Kiyofumi Yumoto⁴

¹ プラズマ、宇宙科学センター 台湾国立成功大学,² 台湾国立成功大学地球科学科,³ 台湾国立成功大学物理学科,⁴ 九州 大学

¹Plasma and SpaceSscience Center, National Cheng kung university, ²Department of Earth Science, National Cheng Kung University, ³Department of Physics, National Cheng Kung Unibersity, ⁴Kyushu University

成層圏の突然昇温が電離圏に影響を及ぼすことが報告されてきた。ここでは2009年の成層圏突然昇温時の電離圏への影響を北半球に限って、今まで報告されていない西経30度 東経30度の領域で調べた。この領域はSSW期間中、10hP高度での大気温度が高かった領域である。使用したデータは台湾のGPS衛星により得られた電子密度の高度分布である。このデータの信頼性を検証するためにイオノゾンデによるNmF2,GIMのTECデータを用い、最終的にデータが研究にたえうることを確認した。

低緯度におけるNmF2は朝9-12時をのぞいてSSW期間中減少する。中緯度にNmF2の変わらない領域が存在する。この場所は中性ガス温度の変化が見られない領域と一致する。高緯度においては昼間はNmF2が増加するが、夜は減少する。

SSW期間中低緯度において6-9時の時間帯にNmF2が大きく減少する期間がある。この時高緯度ではNm F2の上昇がみられる。この現象は赤道以上と同じように、低緯度において、プラズマの強い上昇がおこり、より高い 高度に押し上げられたプラズマが磁力線に沿ってより高緯度に流れ込むとして説明できるかもしれない。

同じような、減少が西経150度、東経150度の経度領域にもみられる。このry等域は成層圏の温度が同じ時期 に上昇している領域であり、西経30度 東経30度にみられる現象はSSWに共通な現象かもしれないことを示唆し ている。この確認のためには2010年のSSWを研究する必要がある。

キーワード: 最大電子密度, コスミック, 成層圏突然昇温, 電離圏, プラズマドリフト Keywords: NmF2, COSMIC, SSW, Ionosphere, Plasma Drift



(May 19-24 2013 at Makuhari, Chiba, Japan)

©2013. Japan Geoscience Union. All Rights Reserved.

PEM06-24

会場:304



時間:5月22日10:05-10:25

Seasonal and Local Time Variation of Ionospheric Migrating Tides in 2007-2011 FORMOSAT-3/COSMIC and TIE-GCM TEC Seasonal and Local Time Variation of Ionospheric Migrating Tides in 2007-2011 FORMOSAT-3/COSMIC and TIE-GCM TEC

Loren Chang^{1*}, Charles Lin², Jann-Yenq Liu¹, Nanan Balan¹, Jia Yue³, Jia-Ting Lin² Loren Chang^{1*}, Charles Lin², Jann-Yenq Liu¹, Nanan Balan¹, Jia Yue³, Jia-Ting Lin²

¹Institute of Space Science, National Central University, Taiwan, ²Department of Earth Science, National Cheng Kung University, Taiwan, ³Atmospheric and Planetary Science Department, Hampton University, USA ¹Institute of Space Science, National Central University, Taiwan, ²Department of Earth Science, National Cheng Kung University, Taiwan, ³Atmospheric and Planetary Science Department, Hampton University, USA

In this study, we examine the seasonal and interannual variation of the major migrating tidal components in total electron content (TEC) observations from the FORMOSAT-3/COSMIC GPS occultation satellite constellation from 2007 through 2011, and their contributions to local time variation in the mid- to low latitudes. We find that the zonal time mean TECs as well as the absolute amplitudes of all of the examined tidal components show a strong positive relation to changes in F10.7 due to the 11 year solar cycle. The relative importance of these components to the local time variation of the ionosphere away from maximum background values differs, with the relative amplitudes of DW1 and TW3 components inversely related to solar activity, while SW2 shows some signs of positive correlation. The features of ionospheric local time variation produced by individual migrating tidal components are consistent from year to year, with DW1 forming the equatorial daytime peak in TEC, SW2 corresponding to the generation of the equatorial ionization anomaly (EIA) crests, and TW3 contributing to the equatorial TEC trough. Numerical experiments using TIE-GCM are also performed to determine the sensitivity of the ionospheric migrating tides to upwards propagating migrating tidal components from the neutral mesosphere and lower thermosphere (MLT). The zonal time mean TECs decrease when MLT tidal forcing is applied, and are particularly sensitive to the MLT DW1. The majority of the ionospheric SW2 response is attributable to the MLT SW2 component, and enhances the poleward shift of the EIA crests by amplifying the equatorial fountain. TW3 in the model is generated through both in-situ photoionization and nonlinear interaction between DW1 and SW2.

 $\neq - \nabla - F$: FORMOSAT-3/COSMIC, TIEGCM, atmospheric tides, migrating tides, ionosphere, mesosphere lower thermosphere

Keywords: FORMOSAT-3/COSMIC, TIEGCM, atmospheric tides, migrating tides, ionosphere, mesosphere lower thermosphere

(May 19-24 2013 at Makuhari, Chiba, Japan)

©2013. Japan Geoscience Union. All Rights Reserved.

PEM06-25

会場:304



時間:5月22日10:25-10:45

Annual/Semiannual Variation in the Thermosphere and Ionosphere Annual/Semiannual Variation in the Thermosphere and Ionosphere

Liying Qian^{1*}, Stanley C. Solomon¹, Alan G. Burns¹, Wenbin Wang¹ Liying Qian^{1*}, Stanley C. Solomon¹, Alan G. Burns¹, Wenbin Wang¹

¹High Altitude Observatory, National Center for Atmospheric Research ¹High Altitude Observatory, National Center for Atmospheric Research

Thermosphere neutral density derived from long-term satellite drag data exhibits an annual/semiannual variation, with maxima near the equinoxes, a primary minimum during northern hemisphere summer, and a secondary minimum during southern hemisphere summer. This annual/semiannual variation is also evident in thermosphere composition (O/N2) measured by the Global Ultraviolet Imager (GUVI) instrument on the TIMED satellite. Recently, we obtained climatology of the daytime peak density and height of the ionospheric F2-region GPS radio occultation measurements by the Constellation Observing System for Meteorology, Ionosphere, and Climate (COSMIC) for the years 2007?2010. The COSMIC data shows that low-latitude NmF2 was dominated by annual/semiannual variations, where NmF2 had maxima near the equinoxes, a primary minimum near the June solstice, and a secondary minimum near the December solstice, and that these annual/semiannual variations extended to mid-latitudes. These thermosphere and ionosphere measurements were compared to simulations by the NCAR Thermosphere-Ionosphere-Electrodynamics General Circulation Model (TIE-GCM). Model reproduction of the annual/semiannual variations in both the thermosphere and ionosphere was significantly improved by imposing seasonal variation of eddy diffusion at the lower boundary. Eddy diffusion represents turbulent mixing processes, which are mainly caused by gravity wave breaking in the mesopause region. These gravity waves are generated in the troposphere, propagate upward, and break in this region. Since changes in turbulent mixing processes affect both the thermosphere and ionosphere by altering the proportion of atomic and molecular gases, the consistent results support the proposition that lower atmospheric forcing can change composition in the thermosphere, and this composition change is a major driver of the annual/semiannual variation in both the neutral and ionized components of the coupled system.

 $\pm - \nabla - F$: thermosphere/ionosphere, neutral density/neutral composition, F2 peak electron density, annual/semiannual variation, eddy diffusion, gravity wave breaking

Keywords: thermosphere/ionosphere, neutral density/neutral composition, F2 peak electron density, annual/semiannual variation, eddy diffusion, gravity wave breaking

(May 19-24 2013 at Makuhari, Chiba, Japan)

©2013. Japan Geoscience Union. All Rights Reserved.

PEM06-26



時間:5月22日11:00-11:15

The response of thermosphere and ionosphere to forcing by geomagnetic activity and lower atmospheric waves The response of thermosphere and ionosphere to forcing by geomagnetic activity and lower atmospheric waves

Wenbin Wang^{1*}, Alan Burns¹, Liying Qian¹, Satn Solomon¹ Wenbin Wang^{1*}, Alan Burns¹, Liying Qian¹, Satn Solomon¹

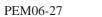
¹High Altitude Observatory, National Center for Atmospehric Research ¹High Altitude Observatory, National Center for Atmospehric Research

The National Center for Atmospheric Research-Thermosphere Ionosphere Electrodynamics General Circulation Model (RTIEGCM) was run to simulate the response of thermosphere wind and temperature to changes in solar-terrestrial environment. We first investigate thermosphere-ionosphere response to variations in the energy and momentum inputs from the magnetosphere under various solar wind conditions. It is found that there were significant enhancements of the westward neutral winds at low and middle latitudes around 190 km during and after a storm. A diagnostic analysis of the model outputs shows that momentum advection from high latitudes to low and middle latitudes was the major cause of these neutral wind changes and that the specific altitude range in which these changes occurred was related to the height distribution of the total momentum forcing. We then examine the day-to-day variability of the ionosphere to study its correlation with geomagnetic activity and lower atmospheric activity forcing at high latitudes, with the day-to-day variability having similar spectral peaks as those in solar-wind and geomagnetic activity. At the geomagnetic equator and in the equatorial-anomaly region, the ionosphere showed more complicated day-to-day variability, suggesting the effect of the interplay of the nonlinear interaction between geomagnetic activity and lower atmospheric waves.

 $\neq - \nabla - F$: Neutral wind, Neutral temperature, Ionospheric density Keywords: Neutral wind, Neutral temperature, Ionospheric density

(May 19-24 2013 at Makuhari, Chiba, Japan)

©2013. Japan Geoscience Union. All Rights Reserved.



会場:304

時間:5月22日11:15-11:30

Study of ionosphere-thermosphere coupling using the SuperDARN Hokkaido radar Study of ionosphere-thermosphere coupling using the SuperDARN Hokkaido radar

西谷 望^{1*}, 小川 忠彦², 行松 彰³, 堤 雅基³, 窄山勝也¹ Nozomu Nishitani^{1*}, Tadahiko Ogawa², Akira Sessai Yukimatu³, Masaki Tsutsumi³, Katsuya Sakoyama¹

¹STEL, Nagoya Univ., ²NICT, ³NIPR
¹STEL, Nagoya Univ., ²NICT, ³NIPR

The SuperDARN Hokkaido (East) radar has been operating for more than 6 years, and yielding many new scientific findings. Several of them are related to ionosphere-upper atmosphere coupling such as traveling ionospheric disturbances (TIDs), coseismic ionospheric disturbances and so on. One of the recent topics is the retrieval of neutral wind velocity in the mesosphere and lower thermosphere, using meteor trail echoes. In this paper, latest result of the study of ionosphere-thermosphere coupling using the SuperDARN Hokkaido (East) radar, together with the progress report of the newly funded Hokkaido West radar, will be presented.

 $\neq - \nabla - F$: SuperDARN Hokkaido radar, ionosphere-thermosphere coupling, TID, coseismic disturbance, neutral wind, midlatitude ionosphere

Keywords: SuperDARN Hokkaido radar, ionosphere-thermosphere coupling, TID, coseismic disturbance, neutral wind, midlatitude ionosphere

(May 19-24 2013 at Makuhari, Chiba, Japan)

©2013. Japan Geoscience Union. All Rights Reserved.

PEM06-28

会場:304



時間:5月22日11:30-11:45

Lithium Release Experiments in the Thermosphere Lithium Release Experiments in the Thermosphere

Shigeto Watanabe^{1*}, Takumi Abe², yuuki furuta¹, Yoshihiro Kakinami³, Masa-yuki Yamamoto³ Shigeto Watanabe^{1*}, Takumi Abe², yuuki furuta¹, Yoshihiro Kakinami³, Masa-yuki Yamamoto³

¹Hokkaido University, ²JAXA/ISAS, ³Kochi University of Engineering ¹Hokkaido University, ²JAXA/ISAS, ³Kochi University of Engineering

Neutral wind in the thermosphere is one of the key parameters to understand the ionosphere-thermosphere coupling process. JAXA/ISAS launched successfully S-520-23 and S-520-26 sounding rockets from Kagoshima Space Center (KSC) on September 2, 2007 and January 12, 2012, respectively. The rocket experiments are called WINDs (Wind measurement for Ionized and Neutral atmospheric Dynamics study) Campaign. The purpose is to investigate the momentum transfer between neutral atmosphere and plasma in the thermosphere and ionospheric E and F-regions. The rocket has installed Lithium Ejection System (LES) as well as instruments for plasma drift velocity, plasma density and temperature and electric and magnetic fields. The atomic Lithium gases were released at altitudes between 150km and 300km in the evening for S-520-23 and at altitude of ~100km in the morning for S-520-26. The Lithium atoms were scattering sunlight by resonance scattering with wavelength of 670nm. The neutral winds and atmospheric gravity waves in the thermosphere were estimated from the movements of Lithium clouds observed by CCD imagers on ground. From the diffusion of Lithium clouds, we estimated neutral density and temperature in the thermosphere. In this presentation, we will include the initial results of Lithium release experiments in Kwajalein EVEX campaign by US-Japan collaborating rocket experiments.

 $+- \nabla - F$: ionosphere, thermosphere Keywords: ionosphere, thermosphere

(May 19-24 2013 at Makuhari, Chiba, Japan)

©2013. Japan Geoscience Union. All Rights Reserved.

PEM06-29



時間:5月22日11:45-12:00

昼間および月明条件下のリチウム放出実験のための S/N 推定 S/N estimation for Lithium release experiments under daytime and moonlight conditions

山本 真行^{1*}, Miguel F. Larsen², 阿部 琢美³, 羽生 宏人³, 渡部 重十⁴, 山本 衛⁵ Masa-yuki Yamamoto^{1*}, Miguel F. Larsen², Takumi Abe³, Hiroto Habu³, Shigeto Watanabe⁴, Mamoru Yamamoto⁵

¹ 高知工科大学, ²Clemson University, ³JAXA 宇宙科学研究所, ⁴ 北海道大学, ⁵ 京都大学生存圈研究所 ¹Kochi University of Technology, ²Clemson University, ³ISAS/JAXA, ⁴Hokkaido University, ⁵RISH, Kyoto University

In order to measure thermospheric wind profile, chemical release experiments by sounding rockets have been used in these decades. Tri-methyl-aluminum (TMA) is usually used in E-region wind measurements, however, for the F-region altitude, it cannot be adapted because of its fast diffusion in the upper thermosphere higher than 160 km. One of the promising methods to measure the F-region wind profile is chemical release of Lithium. The Lithium release has an advantage for its brightness with sunlit condition at a target altitude range, but in a dark sky condition on ground. Thus, we have conducted the Lithium release experiments by using JAXA sounding rockets in these years under twilight sky conditions in evening and dawn. However, the advantage of using Lithium can be extended to the daytime and midnight conditions, when good S/N of the Lithium emission can be proven.

In 2011, we tried to measure the Lithium emission in daytime by using a NASA sounding rocket at Wallops islands, Virginia (VA), U.S., but it failed. The problem has been gradually understood by ground tests and estimation and it might be occurred by failure of Lithium release itself by the on-board Lithium Ejection System (LES) as well as unexpected dense haze over east coast of VA. By improving the LES especially for its burning system by Termite reaction as well as newly applying a small airplane of NASA (named NASA-8) for photographing from 7,500 m altitude, we conducted a test experiment by using NASA Terrior-Improved-Orion sounding rocket (41.107).

The Lithium release experiment of the test flight rocket was successful. Based on the preliminary analyses, the emission in an altitude range of 115-130 km was brighter than 1.5 MR that was obtained by the WIND-1 campaign in Japan at about 230 km altitude. In Japan, we have a plan to observe midnight wind profile at about 200 km altitude by using moonlight of full moon condition with using an airplane of JAXA in summer of 2013. In this talk, we will introduce our results and findings for Lithium release experiments and the S/N of the imaging will be discussed.

キーワード: リチウム放出, 観測ロケット, 熱圏中性風, S/N 比 Keywords: Lithium release, sounding rocket, thermospheric neutral wind, S/N ratio

(May 19-24 2013 at Makuhari, Chiba, Japan)

©2013. Japan Geoscience Union. All Rights Reserved.

PEM06-30

会場:304



時間:5月22日12:00-12:15

Improvement of Retrieval Accuracy of Ionospheric E Region Electron Density from GPS Radio Occultation Technique for COSM Improvement of Retrieval Accuracy of Ionospheric E Region Electron Density from GPS Radio Occultation Technique for COSM

Yen-Hsyang Chu^{1*}, Ching-Lun Su¹ Yen-Hsyang Chu^{1*}, Ching-Lun Su¹

¹Institute of Space Science, National Central University ¹Institute of Space Science, National Central University

It is widely accepted that the use of GPS radio occultation (RO) technique to retrieve ionospheric E region electron density suffers major disadvantage of considerably large retrieval error. In this study, we propose a method to significantly reduce the GPS RO retrieval error of the ionospheric E region electron density. On the basis of IRI model and orbital data of the COSMIC satellites, we first calculate the calibrated total electron content of the GPS signal piercing through the IRI model. The calibrated total electron contents for IRI model during the simulated radio occultation of the COSMIC satellites are then converted into the electron density profile in accordance with Abel transformation. The simulated retrieval errors of the E region electron density of the IRI model are estimated by calculating the difference of the electron densities between IRI model and the simulated GPS RO retrieval. After subtracting the simulated IRI retrieval error from COSMIC-measured electron density, we find that the resultant E region electron density can be greatly improved by a factor ranging from 1.5 to 8, depending on season and geomagnetic latitude region.

 $\neq - \neg - arkappa$: GPS Radio Occultation, E Region Electron Density, Retrieval Error, IRI Model Keywords: GPS Radio Occultation, E Region Electron Density, Retrieval Error, IRI Model

(May 19-24 2013 at Makuhari, Chiba, Japan)

©2013. Japan Geoscience Union. All Rights Reserved.

PEM06-31



時間:5月22日12:15-12:30

Relation between the local equatorial electrojet and global Sq current calculated from different longitude sectors Relation between the local equatorial electrojet and global Sq current calculated from different longitude sectors

Nurul Shazana Abdul Hamid¹*, Huixin Liu¹, Teiji Uozumi², Kiyohumi Yumoto² Nurul Shazana Abdul Hamid¹*, Huixin Liu¹, Teiji Uozumi², Kiyohumi Yumoto²

¹Graduate School of Science, Department of Earth and Planetary Sciences, Kyushu University, Japan, ²International Center for Space Weather Science and Education (ICSWSE), Kyushu University, Japan

¹Graduate School of Science, Department of Earth and Planetary Sciences, Kyushu University, Japan, ²International Center for Space Weather Science and Education (ICSWSE), Kyushu University, Japan

The equatorial electrojet (EEJ) is a strong eastward current flowing in a narrow band along the magnetic dip equator. This current interacts with the global Sq current before decreases to zero near 3 degree dip latitude at both hemispheres. In this study, we examined the relation between the local EEJ component and global Sq current component obtained using two stations method. Analysis was carried using the new equatorial electrojet index, EUEL, calculated from geomagnetic northward, H, component from different longitude sectors. The magnetic EEJ strength is calculated as the difference between the EUEL index of the magnetic dip equator station located beyond EEJ band. The global Sq component is then obtained by subtracting the EEJ component from the EUEL index. Long term data from 2005-2011 are used in this study. The relation between these currents components. The result shows that the amplitude of local EEJ component is always higher than the global Sq component. The second aspect is the day to day variation of these currents obtained from auto-correlation function. The third aspect is the dependence on solar activity represented by the 10.7cm solar radio flux (F10.7). The F10.7-EEJ correlation is found to be slightly higher in 2011 compare to other years. The last aspect is the longitudinal dependence where a comparison is made between the mean of daily amplitude of both currents from different longitude sectors.

 $\neq - \nabla - F$: equatorial electrojet, Sq current, EUEL index, F10.7, correlation analysis Keywords: equatorial electrojet, Sq current, EUEL index, F10.7, correlation analysis

(May 19-24 2013 at Makuhari, Chiba, Japan)

©2013. Japan Geoscience Union. All Rights Reserved.

PEM06-32



時間:5月22日12:30-12:45

赤道ジェット電流とMTI領域中性風との関係 Global characteristics between the EEJ and neutral wind in the MTI region

阿部 修司¹*, 新堀 淳樹², 谷田貝 亜紀代², 池田 大輔³, 湯元 清文¹, 津田 敏隆² Shuji Abe¹*, Atsuki Shinbori², Akiyo Yatagai², Daisuke Ikeda³, Kiyohumi Yumoto¹, Toshitaka Tsuda²

¹ 九州大学国際宇宙天気科学・教育センター,² 京都大学生存圏研究所,³ 九州大学システム情報科学研究院 ¹ICSWSE, Kyushu Univ., ²RISH, Kyoto Univ, ³Faculty of Information Science and Electrical Engineering Kyushu Univ.

The equatorial electrojet (EEJ) is a huge eastward current which flows at the dayside equatorial region of the Earth's ionosphere, in a narrow channel (+-3⁵ 5 degrees in latitudinal range). The EEJ current is observed as an enhanced magnetic variation of the horizontal component of geomagnetic field at the dayside magnetic dip equator. The main mechanism of EEJ is an effect of polarization electric field in the E region of the ionosphere at the dip equator caused by the horizontal magnetic field at the magnetic equator [e.g., Forbes, 1981]. In a recent study, many researchers show the results which comes to relationship the neutral wind and EEJ [e.g., Fang et al., 2008, Aveiro et al., 2009]. However, lack of the long-term comparison analysis of geomagnetic field and wind data obtained from ground magnetometer and atmospheric radars, the detailed relationship between the EEJ and neutral wind fluctuations in the mesosphere and lower thermosphere (MLT) regions has not yet been revealed.

In our previous study, we compared the long-term variation of geomagnetic field data obtained from ground magnetometer and neutral wind data obtained from medium frequency (MF) radar. These instruments were located at the equatorial region. As a result, we found that the relationship between the variations of zonal wind and the residual-EEJ showed a clear inverse correlation. Here, the residual-EEJ is defined as the deviation from the second order fitting curve between the EUV flux and the EEJ amplitude. These results suggest that the vertical current (Jz), which is generated by the dynamo action due to the zonal wind perpendicularly across to the background magnetic field, changes the Cowling conductivity derived under the condition of Jz=0. This trend is observed in not only the Asia Pacific region (close to the radar) but also the South Africa region (far from the radar site). We also performed the frequency analysis to quantitatively define the relationship of zonal wind and residual-EEJ, and found that both of the neutral wind and residual-EEJ have almost the same dominant frequency with a small difference. In addition, we perform the comparative analyses with neutral wind data observed from the satellite, and found the neutral wind disturbance has the same dominant frequency around the equatorial region.

To more clarify the relationship of ionosphere-aerosphere coupling at the equatorial region, we analyzed more neutral wind data estimated from the radars (MF, EAR, and meteor), and more magnetometer data observed around the equatorial region. The radars have been operated by Research Institute for Sustainable Humanosphere, Kyoto University, and the magnetometers belong to MAGDAS managed by International Center for Space Weather Science and Education, Kyushu University. The analysis period is from 1990 to the current. In addition, we perform the comparative analyses between the observational and simulation results at the MLT region. These results allow us to solve the Cowling conductivity including the neutral wind effect, and offer new insight into the study of ionosphere-aerosphere coupling at the equatorial region.

Keywords: equatorial electrojet, MF radar, magnetometer, neutral wind, IUGONET

(May 19-24 2013 at Makuhari, Chiba, Japan)

©2013. Japan Geoscience Union. All Rights Reserved.



PEM06-P01

会場:コンベンションホール

Meridional thermospheric winds observed by Fabry-Perot iterferometers and ionosondes at low latitudes Meridional thermospheric winds observed by Fabry-Perot iterferometers and ionosondes at low latitudes

西岡 未知¹*, 丸山 隆¹, 大塚 雄一², 津川 卓也¹, 塩川 和夫², 石橋 弘光¹, 石井 守¹

Michi Nishioka^{1*}, Takashi Maruyama¹, Yuichi Otsuka², Takuya Tsugawa¹, Kazuo Shiokawa², Hiromitsu Ishibashi¹, Mamoru Ishii¹

1(独)情報通信研究機構,2名古屋大学太陽地球環境研究所

¹National Institute of Information and Communications Technology, ²Solar-Terrestrial Environment Laboratory, Nagoya University

It is important to know the thermospheric wind system in order to understand ionosphere-thermosphere coupling system. Observation of thermospheric wind is traditionally done by Fabry-Perot interferometers (FPIs). It is not easy to observe thermospheric wind every night, because FPI observation depends on weather condition and moon phase, and not many FPI observation has been conducted. Instead of FPI observation, some researchers have estimated meridional wind velocities using data from a pair of ionosondes near geomagnetic conjugate points, assuming that the meridional wind is uniform between the two ionosonde stations (transequatorial wind). However, the comparison between meridional wind velocities estimated by ionosondes and those directly measured by FPIs has not been reported. In this presentation, we show the comparison of meridional winds estimated by ionosondes and those observed by FPIs for the first time. We analyzed data of ionosondes and FPIs installed at Chiang Mai [98.9E, 13.0Mlat] in Thailand and Kototabang [100.3E, -10.0Mlat] in Indonesia. They are located approximately at the geomagnetic conjugate points. Although the estimated and observed wind velocities were generally in good agreement on many nights, we found that they were not in good agreement on some nights. In these nights, the assumption that the meridional wind is uniform between the two ionosonde stations would not be valid. We also investigated seasonal dependence of the correlation between the estimated and observed meridional wind seasonal dependence of the correlation between the estimated and observed meridional wind have more convergence / divergence components from May to July. This result suggests that meridional wind have more convergence / divergence components from May to July.

キーワード: 熱圏風, イオノゾンデ共役観測, ファブリ・ペロー干渉計 Keywords: thermospheric wind, ionosonde conjugate observation, Fabry-Perot Intereferometer

(May 19-24 2013 at Makuhari, Chiba, Japan)

©2013. Japan Geoscience Union. All Rights Reserved.



会場:コンベンションホール

時間:5月21日18:15-19:30

5 チャンネル HRO 電波干渉計の開発と流星軌道およびエコー絶対受信強度の計測の 試み Development of a 5ch HRO-IF and a trial of measureing trajectory and absolute reception power of each meteor echo

山本 真行¹*, 大和 忠良¹ Masa-yuki Yamamoto¹*, Tadayoshi Yamato¹

1高知工科大学

¹Kochi University of Technology

Ham-band Radio meteor Observation (HRO) has an advantage of 24-hour continuous data-detection. In Kochi University of Technology (KUT), a 5ch HRO-IF was developed in 2009 and has been observing the meteor appearance position of every meteor echo, with operating an automatic meteor observation system that automatically publishes observational results on web in quasi-real time (Noguchi, 2009). Meteor parameters acquired by the observation system are: time of detection, elevation and azimuth of the echo, and relative intensity. During 2010-2012, we developed a system of meteor trajectory measurement by multiple-sites observation with precise GPS timing and the 5ch HRO-IF. Then, during 2011-2013, we developed a calibration device for measuring absolute reception power of each meteor echo. Since high time resolution is needed for the determinations of meteor trajectories by the multiple-sites simultaneous observation, a program to analyze the reception power trend with tracking a peak frequency of every 0.001 s by quick repetition of FFT was developed by using the IDL. For the determination of absolute reception power of each meteor echo, we developed a signal generator of observation frequency of 53.75 MHz by applying PLL (Phase Locked Loop) circuit with switching attenuator devices from -80 dBm to -120 dBm per 10 dB in every 5 s. The calibration signal is supplied into a receiver once per 10 minutes, then the artificially supplied stepped function is analyzed automatically and determine each meteor echo reception power in dBm by developed software.

In order to verify the observation system of meteor trajectory measurement, we observed meteor echoes during 4-nights active period of Geminids 2011. We tried a simultaneous observation by high sensitivity video instruments (Watec, WAT-100N) and by a combination of the 5ch HRO-IF and multiple-sites HRO. In the period, 71 meteor echoes were detected, however, only 1 simultaneously observed meteor echo at 3 radio sites as well as the camera site was obtained. Though it was only 1 case, the azimuth angles of the meteor trajectory obtained by the both methods were nearly consistent with each other, within an error range of about 5 degrees for direction-determination by the 5ch HRO-IF. For the confirmation of absolute reception power measurement of each meteor echo, we observed meteor echoes in a peak night of Geminids 2012 with multiple-site optical observations, resulting in 101 absolute reception power of echoes of determined in -80 dBm to -125 dBm. In a region between -100 dBm and -120 dBm, within 1 dB accuracy was confirmed by using test calibration signal supplied by a signal generator (Agilent N9342C).

We improved the KUT radio meteor observation system by adding the measurement of each meteor trajectory and reception power, yielding meteor velocity and its plasma line density for each meteor echo, in case all of the parameter can be fixed. In order to verify the system performance we need more dataset to make a statistical approach, however, here we successfully built a forward-scattering meteor radar system with a capability of meteor trajectory and reception power measurement for obtaining physical parameters. In this paper, we will introduce current status of the KUT radio meteor observation system, that all of the instruments/software were developed by students in this decade.

キーワード: 流星, 流星電波観測, 軌道, 絶対受信強度, 較正, 前方散乱

Keywords: meteor, radio meteor observation, trajectory, absolute reception power, calibration, forward scattering

(May 19-24 2013 at Makuhari, Chiba, Japan)

PEM06-P03

©2013. Japan Geoscience Union. All Rights Reserved.



会場:コンベンションホール

Modification of one-dimensional spherical elementary current systems for applying at low/mid latitude Modification of one-dimensional spherical elementary current systems for applying at low/mid latitude

Ryo Deguchi^{1*}, Heikki Vanhamaki², Huixin Liu³, Olaf Amm² Ryo Deguchi^{1*}, Heikki Vanhamaki², Huixin Liu³, Olaf Amm²

¹Department of Earth and Planetary Sciences, Graduate School of Sciences, Kyushu University, ²Finnish Meteorological Institute, Helsinki, Finland, ³Earth and Planetary Science Division, Kyushu University ¹Department of Earth and Planetary Sciences, Graduate School of Sciences, Kyushu University, ²Finnish Meteorological Institute, Helsinki, Finland, ³Earth and Planetary Science Division, Kyushu University

The technique of 1-dimensional spherical elementary current systems (1D SECS) is one way of determining real ionospheric and field-aligned currents (FAC) from magnetic field measurements observed at a low-orbit satellite. The SECS consist of two sets of basis functions that are either divergence-free (DF) or curl-free (CF), and cause poloidal and toroidal magnetic fields, respectively. In previous studies the full 1D SECS method has been applied only at high latitudes, where we can make the simplifying assumption of radial FAC. This way the full ionospheric current distribution (i.e. both DF and CF horizontal currents and field-aligned currents) can be determined. At low/mid latitudes, on the other hand, only DF equivalent current owing in the ionosphere has been determined from ground magnetic field measurements. In this study, the 1D SECS is applied at low/mid latitudes by including dipole geometry for the FAC associated with the CF elementary systems. The modified 1D SECS is tested to determine both DF and CF ionospheric currents and FAC using both synthetic and real data from the CHAMP satellite and comparing these results with the equivalent current obtained from MAGDAS/CPMN ground magnetic data in 210 MM.

 $\neq - \nabla - F$: spherical elementary current system, Ionospheric currents Keywords: spherical elementary current system, Ionospheric currents

(May 19-24 2013 at Makuhari, Chiba, Japan)

©2013. Japan Geoscience Union. All Rights Reserved.



PEM06-P04

会場:コンベンションホール

時間:5月21日18:15-19:30

Atmospheric Density Modeling Using Neural Networks Atmospheric Density Modeling Using Neural Networks

Hongru Chen^{1*}, Huixin Liu², Toshiya Hanada¹ Hongru Chen^{1*}, Huixin Liu², Toshiya Hanada¹

¹Department of Aeronautics and Astronautics, Kyushu University, ²Department of Earth and Planetary Science, Kyushu University

¹Department of Aeronautics and Astronautics, Kyushu University, ²Department of Earth and Planetary Science, Kyushu University

Atmospheric density during geomagnetic storms is usually poorly predicted due to the lack of clear understanding of the coupling mechanism between thermosphere and magnetosphere in such circumstances. Consequently, the orbit prediction in severe geomagnetic condition is affected. Neural networks are the technique of identifying nonlinear system without exactly knowing its physical model. In the present study, an attempt has been made to model the atmospheric density using neural networks. In developing such models, we use both the ring current index Dst and the geomagnetic index ap as model inputs. The ap index is commonly used in density models such as the MSIS and the Jacchia series to represent geomagnetic activity. On the other hand, Dst has been reported to have better correlation with the storm-time density, and to represent additional heating source to that represented by ap. The density data used for modeling is derived from satellites CHAMP and GRACE's accelerometer measurements. The performance of the neural network models (NNMs) is compared with that of the NRLMSISE-00 at different geomagnetic activity level, which reveals the advantages of the neural network technique and the Dst index.

 $\neq - \nabla - F$: Atmospheric density, Neural networks modeling, Geomagnetic storm, Magnetic activity index Keywords: Atmospheric density, Neural networks modeling, Geomagnetic storm, Magnetic activity index

(May 19-24 2013 at Makuhari, Chiba, Japan)

©2013. Japan Geoscience Union. All Rights Reserved.



PEM06-P05

会場:コンベンションホール

Coupling of electrons and inertial Alfven waves in the top-side ionosphere Coupling of electrons and inertial Alfven waves in the top-side ionosphere

Run Shi^{1*}, Huixin Liu¹, Akimasa Yoshikawa¹, Zhang Beichen², Ni Binbin³ Run Shi^{1*}, Huixin Liu¹, Akimasa Yoshikawa¹, Zhang Beichen², Ni Binbin³

¹Department of Earth and Planetary Sciences, Kyushu University, ²SOA Key Laboratory for Polar Science, Polar Research Institute of China, ³Department of Atmospheric and Oceanic Sciences, UCLA

¹Department of Earth and Planetary Sciences, Kyushu University, ²SOA Key Laboratory for Polar Science, Polar Research Institute of China, ³Department of Atmospheric and Oceanic Sciences, UCLA

A one dimensional kinetic model is constructed to simulate the electron acceleration by inertial Alfven waves. The electrons are divided into cold and hot electrons and treated separately. Cold components are described by the fluid equation and hot ones by the Vlasov equation, both carrying field-aligned currents. Intense variation of Alfven speed has been introduced by inclusion of cold electrons. The model results show that the exponential decrease of the plasma density plays a key role, which leads to the sharp gradient of both Alfven velocity and electron inertial length. When Alfven waves encounter this sharp gradient at lower altitudes, the electrons accelerated by the waves become super-Alfvenic, and the width of burst structures becomes much wider than the electron inertial length. Consequently, the background electrons carry the oppositely field-aligned current due to plasma oscillation. It is demonstrated that the current carried by the electrons exceeding the wave front is balanced by the reverse current carried by background electrons. This mechanism can be used to reasonably explain observations of the electron bursts accompanied by little net field-aligned current. Furthermore, our simulation indicates that Alfven wave reflection is modified due to mirror force and wave particle interaction.

 $\neq - \nabla - F$: inertial Alfven waves, super-Alfvenic, bursts Keywords: inertial Alfven waves, super-Alfvenic, bursts Japan Geoscience Union Meeting 2013 (May 19-24 2013 at Makuhari, Chiba, Japan)

©2013. Japan Geoscience Union. All Rights Reserved.



PEM06-P06

会場:コンベンションホール

時間:5月21日18:15-19:30

Adjustment of the ionospheric height for TEC derivation of GRBR network Adjustment of the ionospheric height for TEC derivation of GRBR network

Kornyanat Watthanasangmechai1*, Mamoru Yamamoto1, Akinori Saito2 Kornyanat Watthanasangmechai^{1*}, Mamoru Yamamoto¹, Akinori Saito²

¹Research Institute for Sustainable Humanosphere, Kyoto University, ²Department of Geophysics, Graduate School of Science, Kyoto University

¹Research Institute for Sustainable Humanosphere, Kyoto University, ²Department of Geophysics, Graduate School of Science, Kyoto University

To derive Total Electron Content (TEC) of GNU Radio Beacon Receiver (GRBR) network in low latitude region, the ionospheric height was adjusted to reduce a TEC estimation error. GRBR is a simple digital receiver developed to measure the ionospheric total electron content (TEC) from Low-Earth-Orbit (LEO) satellites. GRBR network is used to capture the smallscale structure of the ionosphere. It is known that fixed altitude of the ionosphere leads to large error of TEC in low latitude sector. In order to reveal a low latitude meridional TEC distribution, we thus developed the method with adjustable ionospheric height to derive GRBR-TEC.

This method employs data from 5 GRBRs, 3 ionosondes and 17 GPS receivers in March 2012. The GRBR receivers are located at Kototabang (0.20S, 100.32E), Phuket (7.89N, 98.38E), Chumphon (10.72N, 99.37E), Bangkok (13.73N, 100.77E), and Chiang Mai (18.76N, 98.93E). The ionsondes are located at Kototabang (0.20S, 100.32E), Chumphon (10.72N, 99.37E) and Chiang Mai (18.76N, 98.93E). The GPS stations distribute from 25N to 10S and 98E to 108E in the geographic coordinate. Assuming that mean ionospheric height variation is a function of latitude, the ionospheric height at each position was adjusted based on an ionosonde-hmF2. Consequently, GPS-TEC was employed as a zero-guess to estimate the bias for the GRBR-TEC calculation. As a result, meridional TEC of the low-latitude ionosphere over equatorial region was obtained with high accuracy for both cases with and without plasma bubble occurrence. In addition, an asymmetry of EIA enhancement was captured as well, which will be discussed in the presentation. The proposed method with adjustable ionospheric height was successful to derived multi-station GRBR-TEC from polar orbit satellite.

キーワード: GRBR-TEC, Ionospheric height, Equatorial region, EIA, Ionosonde, GPS Keywords: GRBR-TEC, Ionospheric height, Equatorial region, EIA, Ionosonde, GPS

(May 19-24 2013 at Makuhari, Chiba, Japan)

©2013. Japan Geoscience Union. All Rights Reserved.



PEM06-P07 会場:コンベンションホール

Observations of seismo-traveling ionospheric disturbance triggered by earthquake and tsunami Observations of seismo-traveling ionospheric disturbance triggered by earthquake and tsunami

Wei-han Chen^{1*}, Charles Lin¹, Chia Hung Chen¹, Huixin Liu² Wei-han Chen^{1*}, Charles Lin¹, Chia Hung Chen¹, Huixin Liu²

¹Department of Earth Sciences, National Cheng Kung University, ²Earth and Planetary Science Division, Kyushu University SERC, Kyushu University

¹Department of Earth Sciences, National Cheng Kung University, ²Earth and Planetary Science Division, Kyushu University SERC, Kyushu University

In this study, the seismo-traveling ionospheric disturbances (STIDs) of total electron content (TEC) generated by the 2011 Mw9.0 Tohoku earthquake at 05:46:23 UT on March 11, 2011, are investigated by using ground-based Global Positioning System (GPS) receiver networks. The STIDs are not only triggered by seismic surface waves but also by tsunami waves of the Tohoku earthquake. A method of wavelet analysis is used to investigate the spectral characters of STIDs induced by seismic surface waves and tsunami waves. Results find that the spectrum of STID by surface waves shows a single short period enhancement, while the spectrum of STID by tsunami waves shows multiple long-period responses. Multiple events, including 1999 Chi-chi, 2003 Hokkaido, 2004 Sumatra, and 2010 Chile earthquakes, are employed to investigate the general spectral characteristics of seismic surface and tsunami waves. This study also find that the arrival time of STID by surface waves is earlier than that by tsunami waves, which could be applied for the short-term tsunami warnings.

 $+- \nabla - F$: ionosphere, STID, tsunami Keywords: ionosphere, STID, tsunami

(May 19-24 2013 at Makuhari, Chiba, Japan)

©2013. Japan Geoscience Union. All Rights Reserved.



会場:コンベンションホール

時間:5月21日18:15-19:30

Variability of the gravity wave forcing from troposphere to mesosphere: By momentum flux estimation Variability of the gravity wave forcing from troposphere to mesosphere: By momentum flux estimation

Eswaraiah Sunkara^{1*}, M. Venkat Ratnam², B.V. Krishna Murthy³, S.Vijaya Bhaskara Rao¹ Eswaraiah Sunkara^{1*}, M. Venkat Ratnam², B.V. Krishna Murthy³, S.Vijaya Bhaskara Rao¹

¹Department of Physics, Sri Venkateswara University, Tirupati-517502, India, ²National Atmospheric Research Laboratory (NARL), Gadanki, Tirupati-517 502, India, ³B1, CEEBROS, Chennai-600020, India. ¹Department of Physics, Sri Venkateswara University, Tirupati-517502, India, ²National Atmospheric Research Laboratory (NARL), Gadanki, Tirupati-517 502, India, ³B1, CEEBROS, Chennai-600020, India.

Using long-term data (1998 to 2008) collected from Mesosphere-Stratosphere-Troposphere (MST) radar and Rayleigh Lidar located at a tropical station, Gadanki (13.50N, 79.20E), India, variability of the gravity wave forcing from troposphere to mesosphere is investigated by estimating the momentum flux associated with the gravity waves of periods 20 min. to 2 h, for the first time. The emphasis is on seasonal variability of mean zonal and meridional momentum fluxes in mesosphere and troposphere and vertical flux of zonal momentum in the stratosphere. An effort is made to examine the variations in momentum flux for different cases, viz., during the occurrence of mesospheric temperature inversion and convection events. At tropospheric altitudes of 11-16 km large enhancement in flux is noticed during equinoxes. In the stratosphere the maximum values of flux (~2.8 m2/s2) are pragmatic in winter and spring at the altitude region 58-62 km. Interestingly, the vertical flux of zonal momentum estimated from lidar is in the range of those estimated from radar data in the overlap altitude region, though the estimates are from two different techniques. In the mesosphere, in summer large variations with altitude in zonal momentum flux are noticed with a magnitude ~0- 4 m2/s2. The meridional fluxes in the mesosphere are higher in equinoxes (~10-12 m2/s2). The two case studies showed that during mesospheric temperature inversion due to large wave breaking at mesosphere, momentum fluxes are raised up to ~7-10 m2/s2 and during deep convection, large variations in troposphere momentum fluxes are noticed than in mesosphere and the variations in mesosphere, the possible reasons are discussed.

 $\neq - \nabla - F$: Mesosphere-Stratosphere-Troposphere, short-period gravity waves, Momentum flux, MST radar, Rayleigh lidar Keywords: Mesosphere-Stratosphere-Troposphere, short-period gravity waves, Momentum flux, MST radar, Rayleigh lidar

(May 19-24 2013 at Makuhari, Chiba, Japan)

©2013. Japan Geoscience Union. All Rights Reserved.



PEM06-P09 会場:コンベンションホール

時間:5月21日18:15-19:30

南極昭和基地の共鳴散乱ライダーシステム: カリウム層の国内試験観測 Resonance scattering lidar system at Syowa Station in Antarctica: Test observations of potassium layer in Japan

津田 卓雄^{1*}, 江尻 省¹, 阿保 真², 川原 琢也³, 中村 卓司¹ Takuo Tsuda^{1*}, Mitsumu Ejiri¹, Makoto Abo², Taku D Kawahara³, Takuji Nakamura¹

¹国立極地研究所,²首都大学東京大学院システムデザイン研究科,³信州大学工学部

¹National Institute of Polar Research, ²Graduate School of System Design, Tokyo Metropolitan University, ³Faculty of Engineering, Shinshu University

We are developing a new resonance scattering lidar system to be installed at Syowa Station (69S, 39E) in Antarctica. For the new lidar system, we have employed a tunable alexandrite laser covering the resonance scattering wavelengths of two neutral species, which are atomic potassium (K, 770.11 nm) and atomic iron (Fe, 386.10 nm), and two ion species, which are calcium ion (Ca⁺, 393.48 nm) and aurorally excited nitrogen ion (N₂⁺, 390.30 nm, 391.08 nm). Thus the new lidar system will provide information on the mesosphere and lower thermosphere as well as the ionosphere. Using the new resonance scattering lidar and other instruments, we will conduct a comprehensive ground-based observation of the low, middle, and upper atmosphere above Syowa Station. This unique observation is expected to make important contribution to studies on the atmospheric vertical coupling process and the neutral and charged particle interaction. In this presentation, we introduce the new resonance scattering lidar system and report current status of its development. In particular, our presentation focus on test observations of potassium layer at National Institute of Polar Research in Tachikawa, Japan.

Keywords: Resonance scattering lidar, Potassium layer, Syowa Station, Antarctica